frontiers | Frontiers in Cellular and Infection Microbiology

TYPE Original Research
PUBLISHED 05 February 2025
DOI 10.3389/fcimb.2025.1513908



OPEN ACCESS

EDITED BY
Martin Craig Taylor,
University of London, United Kingdom

REVIEWED BY
Juan David Ospina-Villa,
Colombian Institute of Tropical Medicine (ICMT), Colombia
Izabela Marques Dourado Bastos,
University of Brasilia, Brazil

*CORRESPONDENCE
Angela K. Cruz
akcruz@fmrp.usp.br

RECEIVED 19 October 2024
ACCEPTED 15 January 2025
PUBLISHED 05 February 2025

CITATION
Quilles JC Jr, Espada CR, Orsine LA, Defina TA, Almeida L, Holetz F and Cruz AK (2025) A short ncRNA modulates gene expression and affects stress response and parasite differentiation in *Leishmania braziliensis*. *Front. Cell. Infect. Microbiol.* 15:1513908. doi: 10.3389/fcimb.2025.1513908



# A short ncRNA modulates gene expression and affects stress response and parasite differentiation in *Leishmania braziliensis*

José C. Quilles Jr[1], Caroline R. Espada[1], Lissur A. Orsine[1], Tânia A. Defina[1], Letícia Almeida[1], Fabíola Holetz[2] and Angela K. Cruz[1]*

[1]Laboratory de Molecular Parasitology, Department of Cell and Molecular Biology, Ribeirão Preto Medical School, FMRP/USP – University of São Paulo, Ribeirão Preto, SP, Brazil, [2]Laboratory of Gene Expression Regulation, Carlos Chagas Institute, Oswaldo Cruz Foundation, Curitiba, PR, Brazil

The protozoan parasite *Leishmania* spp. is a causative agent of leishmaniasis, a disease that affects millions of people in more than 80 countries worldwide. Apart from its medical relevance, this organism has a genetic organization that is unique among eukaryotes. Studies of the mechanisms regulating gene expression in *Leishmania* led us to investigate noncoding RNAs (ncRNAs) as regulatory elements. We previously identified differentially expressed (DE) ncRNAs in *Leishmania braziliensis* with potential roles in the parasite biology and development. Herein, we present a functional analysis of one such DE ncRNA, the 147-nucleotide-long transcript ncRNA97, which is preferentially expressed in amastigotes, the replicative form within mammalian phagocytes. By RT-qPCR the ncRNA97 was detected in greater quantities in the nucleus under physiological conditions and in the cytoplasm under nutritional stress. Interestingly, the transcript is protected at the 5' end but is not processed by the canonical trypanosomatid *trans*-splicing mechanism, according to the RNA circularization assay. ncRNA97 knockout ($^{KO}$) and addback ($^{AB}$) transfectants were generated and subjected to phenotypic analysis, which revealed that the lack of ncRNA97 impairs the starvation response and differentiation to the infective form. Comparative transcriptomics of ncRNA97$^{KO}$ and parental cells revealed that transcripts encoding amastigote-specific proteins were affected. This pioneering work demonstrates that ncRNAs contribute to the developmental regulatory mechanisms of *Leishmania*.

KEYWORDS

**noncoding RNA, leishmania, gene expression, metacyclogenesis, nutritional stress**

# 1 Introduction

Leishmaniasis is a human disease that can be caused by more than 20 species of *Leishmania* parasites worldwide. In South America, *Leishmania* (*Viannia*) *braziliensis* is the most important etiological agent of mucocutaneous leishmaniasis (Queiroz et al., 2012), a severe and morbid tegumentary disease (Rogers et al., 2011). *Leishmania* parasites are transmitted to humans and other mammals through the bite of an infected female sandfly; thus, the parasite lifecycle demands agile adaptation to hostile environments within both vertebrates and invertebrates. Nutritional stress in the sandfly midgut triggers the differentiation of the procyclic form into the infective metacyclic form of the parasite (metacyclogenesis), which is released into the mammalian dermis during a blood meal (Bates, 2007; Silva-Almeida et al., 2012). Inside macrophages, the metacyclic form differentiates into the replicative intracellular amastigote, which multiplies and spreads to other cells, causing tissue damage and inflammation (Saxena et al., 2007).

Compared to other eukaryotes, *Leishmania* kinetoplastids possess a unique genetic organization in which functionally unrelated genes are organized as polycistronic units in 34-36 chromosomes in the absence of canonical promoters. Virtually all mRNAs are polycistronically transcribed by RNA-Pol II and co-transcriptionally processed into mature mRNAs. This is accomplished by *trans*-splicing of the 39 nucleotide long mini-exon (ME) sequence of the capped spliced leader RNA to the 5′ end of the new transcript, coupled with the polyadenylation of the upstream gene (Lebowitz et al., 1993; Ullu et al., 1993; Matthews et al., 1994). The control of gene expression in these parasites involves coordinated mechanisms that respond to specific environmental triggers during the life cycle (De Pablos et al., 2016, 2019). Due to this atypical genome organization, co- and posttranscriptional mechanisms are critical for the control of gene expression in these protozoans (Clayton, 2014, 2016; Martínez-calvillo et al., 2018). The discovery of noncoding RNAs (ncRNAs) that control gene expression in different organisms has raised the question of whether ncRNAs could play a similar role in trypanosomatids. Aside from the housekeeping ncRNAs (tRNAs, rRNA, and snRNAs) (Ernst and Morton, 2013), ncRNAs have diverse functions and can be processed in a range of different ways (Chan and Tay, 2018; Shih et al., 2020). An arbitrary classification of long (> 200 nt) and short (< 200 nt) sequences is frequently used, but specific characteristics, such as genomic localization, molecular interactions, and functions, can also be used (Ernst and Morton, 2013). However, a recent novel classification defines long ncRNAs as those >500 nucleotides long (Mattick et al., 2023). The best studied short noncoding RNAs are microRNAs (miRNAs), which act as *cis*- or *trans*-elements by binding to the 3'-untranslated region (UTR) of a target mRNA and modulating its stability and/or translation (Guo et al., 2010). Despite their short length of only 22 nucleotides, miRNAs play a major role in gene regulation, and their misregulation is connected to a range of human diseases (Ghildiyal and Zamore, 2009; Fernandes et al., 2019).

Although it has been 30 years since the first functional eukaryotic ncRNA was discovered (Brannan et al., 1990), only a few ncRNAs have been detected in trypanosomatids (Iribar et al., 2003; Dumas et al., 2006; Zheng et al., 2013; Freitas Castro et al., 2017; Chikne et al., 2019; Guegan et al., 2022). A small nucleolar ncRNA regulates differentiation in *Trypanosoma brucei* parasites by manipulating the expression of two essential differentiation factors (Guegan et al., 2022). In *Leishmania* parasites, the ncRNA ODD3 emerges from the 3'UTR of only one of the gene copies encoding the ribosomal protein S16 (Freitas Castro et al., 2017), but its function remains unknown. We recently identified approximately 3,600 ncRNAs that are differentially expressed (DE) in different developmental stages of *Leishmania braziliensis* (Ruy et al., 2019) in an effort to understand the possible functions and relevance of these ncRNAs in life cycle regulation. Here, we characterized one of these DE ncRNAs and showed that it modulates the expression of a group of genes and that it is involved in the regulation of the nutritional stress response and in metacyclogenesis, an essential differentiation process for parasite development.

# 2 Materials and methods

## 2.1 Cell culture, *in vitro* differentiation, and infection assays

Promastigotes of the *Leishmania braziliensis* strain M2903 (MHOM/BR/75/M2903) expressing tdTomato fluorescent protein (Lorenzon et al., 2022) were cultured in M199 medium (Sigma-Aldrich) supplemented with 10% heat-inactivated fetal bovine serum (FBS) as previously described (Kapler et al., 1990). For the metacyclogenesis assay, $10^5$ parental and knockout cells·mL-1 were incubated in 10 mL of M199 medium and grown for 120 h. Then, the metacyclic fraction was enriched by Ficoll, as described (Späth and Beverley, 2001). The total number of cells before purification was set as 100%, and the percentage of the metacyclic form recovered was used to estimate the differentiation rate. Purified metacyclic parasites were used to infect THP-1 human macrophages *in vitro*. THP-1 monocytes were cultivated in RPMI medium at 37°C in a 5% $CO_2$ atmosphere and differentiated inside macrophages in 96-well black flat-bottom plates at $2{\cdot}10^4$ cell·$mL^{-1}$ according to an established protocol (Daigneault et al., 2010). After differentiation, the purified metacyclic forms were incubated at a ratio of 10:1 with macrophages for 4 h. Afterward, the cells were double-washed with PBS and incubated with RPMI medium for 48 h at 33°C in a 5% $CO_2$ atmosphere. The nuclei were stained with 0.25% Hoechst (Merck-Millipore), and images were taken for 9 fields of view in each well under 40x magnification by the ImageXpress Micro XLS System (Molecular Devices, LLC, USA) using DAPI and Texas Red filters. The infectivity rate (%) and intracellular amastigote growth were obtained as described in a previous publication (Lorenzon et al., 2022). To obtain axenic amastigotes for the oxidative stress assay, $10^5$ metacyclic promastigotes purified from the Ficoll assay were incubated in 5 mL of 100% FBS and incubated at 33°C in a 5% $CO_2$ atmosphere for 72 h. Afterward, one passage of the axenic amastigotes was performed before using the cells for assays. Stage-specific markers were tested for both metacyclic and amastigote morphologies as described previously (Ruy et al., 2019).

## 2.2 Transfection to generate knockout and add-back parasites

The production of single guide RNA and donor DNA templates for knockout parasite generation followed the protocol from Beneke et al., 2017. After DNA recovery by ethanol precipitation, promastigotes in the log phase expressing the Cas9 endonuclease were transfected as previously described (Lorenzon et al., 2022). Knockout ($^{KO}$) parasites were selected in the presence of puromycin as the selection marker, and edited homozygotes were confirmed by conventional PCR (see Supplementary Figure 3B) and total RNA-seq analysis, comparing knockout and parental cell lines. For FtsX-like$^{KO}$ confirmation, conventional PCR and RT-qPCR were applied (see section 2.3). For add-back ($^{AB}$) parasites, a plasmid was used to clone the ncRNA97 sequence (see Supplementary Figure 5). Then, $10^7$ ncRNA97$^{KO}$ parasites were transfected with 30 µg of plasmid and selected under drug pressure on solid culture media. Approximately 15 individual parasite colonies were collected after transfection, and plasmid insertion was confirmed by conventional PCR targeting the drug resistance region (streptothricin acetyltransferase – SAT).

## 2.3 RNA extraction and RNA-seq data generation

Total RNA was extracted from parasites of different morphologies with a Direct-zol extraction kit (Zymo Research). RNA samples were quantified by UV–Vis, and the quality was evaluated with an Agilent Bioanalyzer system (RNA 600 Nano kit – Agilent, Waldbronn, Germany) according to the manufacturer's instructions. Then, RNA samples were subjected to qPCR and circularization assays. For RNA-seq data generation, total RNA from procyclic promastigotes in biological triplicates was rRNA depleted using a Ribo-Zero Plus rRNA Depletion Kit (Illumina). RNA sequencing was carried out by BGI (https://www.bgi.com/global) using a DNBSEQ Eukaryotic Strand-specific mRNA Library Preparation Kit (poly(A) tail capture and strand-specific) and the DNBseq sequencing platform (paired-end reads). After data pretreatment conducted by BGI (adapters and low-quality read removal), approximately 70 million reads per library remained. Reads were mapped to the *Leishmania braziliensis* MHOM/BR/75/M2903 genome (TriTrypDB version 56, https://tritrypdb.org/tritrypdb/app/) with Bowtie2 (version 2.3.2) (Langmead and Salzberg, 2012) and the additional parameters -local and -N1. Next, reads mapped to each gene locus were counted with HTSeq-count (version 0.12.4) (Putri et al., 2022) using the additional parameters *–nonunique=all*, *–stranded=reverse*, *–order=pos* and *–mode=union*. Differential gene expression analysis was conducted using the R Bioconductor DESeq2 package (version 1.20.0) (Love et al., 2014), and genes were considered differentially expressed when $p$-value adjusted < 0.05. An additional fold-change cutoff (FC > 1.5) was applied to prioritize genes with greater differences in expression levels between groups.

## 2.4 Circular RNA assay

Total RNA extracted from log phase promastigotes was used for the determination of the 5' and 3' ends of the ncRNA97 transcripts following a previously published protocol (Hang et al., 2015). Briefly, 1 µg of total RNA was treated or not treated with 1,000 U of tobacco acid pyrophosphatase (TAP) at 37°C for 1 h to generate 5'-monophosphate RNAs. Then, RNA circularization was performed using 3,000 U of T4 RNA ligase for 2 h at 37°C. Total RNA was precipitated with ethanol and recovered in 70 µL of RNAse-free water. This precipitated RNA was used to generate complementary DNA (cDNA) by reverse transcription using a gene-specific primer (cRT), followed by amplification of the region of interest by conventional PCR using specific primers for the ncRNA97 sequence (cF1/cR1 and cF2/cR2), which was directed outward of the transcript in each extremity. The amplicon was purified and cloned and inserted into a pGEM-T Easy vector. After RNA circularization, colony PCR was performed on 5 colonies for each amplicon, and the products of different sizes were sequenced. The results were analyzed with Geneious Prime Software. Details about the primer sequences, colony PCR gel, and transcript sequences are provided in Supplementary Figure 1.

## 2.5 Reverse transcription quantitative PCR

After RNA extraction, total RNA was treated with DNase Turbo (Thermo Fisher Scientific), and an RT–qPCR assay was performed as previously described (Ruy et al., 2019). The data were analyzed according to the ΔΔCt method (Pfaffl, 2001) using the geometric mean of two selected housekeeping genes (G6PD or 7SL) for normalization according to a previously described strategy (Vandesompele et al., 2002). The RT–qPCR data were analyzed using GraphPad Prism 5 (Prism). The data shown correspond to the means and standard deviations (± SDs) from 3 independent experiments. The primers used in this study were as follows: ncRNA97 Fw 5'-GTTGGTAATCGTGTGAGTGTGTG-3', Rv 5'-GTGGTGTTTGGTAGGACGGT-3'; Amastin (LBRM2903_080014000) Fw: 5'-CCTTGCGCTCAACATCACTG-3', Rv: 5'-AACCAGGCCACCACAAACAT-3'; Amastin (LBRM2903_100024300) Fw: 5'-CCTTCTTGGGAGTCGGCTTC-3', Rv: 5'-CTTCTACTTCCCCTCGCTGC-3'; Stress-induced (LBRM2903_080016600) Fw: 5'-AGGGAGTGAAAGACGTGCAG-3', Rv: 5'-TCAGGTTGCAGCATCAGGAG-3'; core histone (LBRM2903_3500053000) Fw, 5'-CCGCCGTGACTGTCTTCTT-3'; Rv, 5'-GGTGGTGTAAAGCGCATCTC-3'; and DEAD/DHA helicase (LBRM2903_3200217000) Fw 5'-CATACACGAGCGACACCGTA-3', Rv 5'-CGTGTGGAGTCCGTGAAGAA-3'. For ncRNA intracellular localization, total RNA was fractionated following the Ambion™ Paris™ system instructions (Invitrogen) already used for noncoding RNAs separation in *Plasmodium falciparum* (Batugedara et al., 2023). Briefly, total RNA was extracted from a pool of cells with Trizol and used for the fractionation using the RNA-affinity column and buffers supplied by Invitrogen. After that, RNA samples were treated with

DNAse and submitted to RT-qPCR using the same method and primers already described.

## 2.6 Exonuclease treatment

Total RNA treated with DNase Turbo (Thermo Fisher Scientific) was incubated with the XRN-1 (NEB) 5'➔ 3' exoribonuclease to degrade 5'-monophosphate transcripts. For that, 1 µg of RNA was previously treated with 1,000 U of MDE (mRNA decapping enzyme – NEB) at 37°C for 2h, precipitated overnight with ethanol, followed by treatment of 1,000 U of XRN-1 at 37°C for 2 h. Then, RNA was again precipitated with ethanol and used for cDNA generation by reverse transcription. The presence of the ncRNA97 transcript was confirmed by conventional PCR and detected on a 1.5% agarose gel. For the positive control, genomic DNA was used. An RNA sample not subjected to reverse transcription was used as a negative control to confirm DNA degradation by DNase. The sequences of the primers used were 5'-3' Fw_GTTGGTAATCGTGTGAGTGTGTG and Rv_GTGGTGTTTGGTAGGACGGT.

## 2.7 Secondary RNA structure determination

Secondary structures of the single-stranded RNA were predicted by the RNAfold WebServer (Gruber et al., 2008) with the minimum free energy (MFE) and partition function algorithms from the Turner model (Mathews, 2014). All sequenced transcripts for ncRNA97 found in the circularization assay were subjected to secondary structure prediction.

## 2.8 Pulldown assay – *in vitro* RNA–protein interaction

The sequences corresponding to the predicted ncRNA97 sequence were amplified from the genomic DNA using the primers Fw (5'-CGTTGTTGGTAATCGTGTGAGT-3') and Rv (5'-AGTGGTGTTTGGTAGGACG-3'). Then, it was cloned and inserted into a pUC-56 plasmid between the T7 promoter and 4xS1m aptamer sequences, adapted from Leppek's strategy (Leppek and Stoecklin, 2014). RNA was transcribed *in vitro* (MEGAscript T7 transcription kit – Thermo Fisher AM1334), and 10 µg of purified RNA was immobilized on streptavidin magnetic beads (NEB) for 8 h at 4°C under orbital rotation in binding buffer (24 mM KCl, 10 mM Tris-base pH 7.8, and 10 mM MgCl2). All experiments were performed in an RNAse-free environment with diethylpyrocarbonate (DEPC) pretreatment and the addition of RNAse inhibitors (200 U). An empty sequence between the T7 promoter and 4xS1m aptamer was used as an RNA control to identify nonspecific partners. A total of $10^8$ parasites were lysed in 1 mL of SA-RNP-Lyse buffer (20 mM Tris-HCl pH 7.5, 150 mM NaCl, 1.5 mM MgCl2, 2 mM DTT, 2 mM RNase inhibitor, 1 protease inhibitor cocktail tablet (Merck), 1% Triton X-100) on ice with physical pressure using a 19 G needle. Biotinylated proteins were removed from the extract by incubating the lysed extract for 8 h at 4°C with streptavidin beads. Subsequently, the supernatant was incubated with the bead-immobilized wild-type ncRNA97 sequence for 8 h at 4°C. Afterward, the beads were washed three times with wash buffer (20 mM Tris-HCl pH 7.5, 300 mM NaCl, 5 mM MgCl2, 2 mM DTT, 2 mM RNase inhibitor, and 1 protease inhibitor cocktail tablet), resuspended in 35 µL of Laemmli buffer (Laemmli, 1970) and boiled for 10 min before being applied to a 12% polyacrylamide gel. Electrophoresis was run at 110 V until the samples reached the separation gel.

## 2.9 Proteomic analysis, mass spectrometry, database search, and protein identification criteria

Protein digestion and mass spectrometry analyses were performed by the Proteomics Platform of the CHU de Québec Research Center (Quebec, QC, Canada). Gel bands from the samples were sent for protein identification by mass spectrometry analysis and three biological replicates were evaluated for the ncRNA97 sequence and the control. Bands of interest were extracted from gels and placed in 96-well plates and washed with water. Proteins were reduced with 10 mM DTT and alkylated with 55 mM iodoacetamide. Trypsin digestion was performed using 126 nM of modified porcine trypsin (Sequencing grade, Promega, Madison, WI) at 37°C for 18 h. Digestion products were extracted using 1% formic acid, 2% acetonitrile followed by 1% formic acid, 50% acetonitrile. The recovered extracts were pooled, vacuum centrifuge dried, and then resuspended into 10 µL of 0.1% formic acid, and 5 µL were analyzed by mass spectrometry.

Mass Spectrometry. Samples were analyzed by nano LCMS/MS using a Dionex UltiMate 3000 nanoRSLC chromatography system (Thermo Fisher Scientific) connected to an Orbitrap Fusion mass spectrometer (Thermo Fisher Scientific, San Jose, CA, USA). Peptides were trapped at 20 µL/min in loading solvent (2% acetonitrile, 0.05% TFA) on a 5 mm × 300 µm C18 pepmap cartridge precolumn (Thermo Fisher Scientific/Dionex Softron GmbH, Germering, Germany) during 5 min. Then, the precolumn was switched online with a Pepmap Acclaim column (Thermo Fisher) 50 cm × 75 µm internal diameter separation column and the peptides were eluted with a linear gradient from 5 to 40% solvent B (A: 0.1% formic acid, B: 80% acetonitrile, 0.1% formic acid) in 200 min, at 300 nL/min. Mass spectra were acquired using a data dependent acquisition mode using Thermo XCalibur software version 4.3.73.11. Full scan mass spectra (350 to 1800 m/z) were acquired in the Orbitrap using an AGC target of $4 \times 10^5$, a maximum injection time of 50 ms, and a resolution of 120 000. Internal calibration using lock mass on the m/z 445.12003 siloxane ion was used. Each MS scan was followed by MS/MS fragmentation of the most intense ions for a total cycle time of 3 s (top speed mode). The selected ions were isolated using the quadrupole analyzer in a window of 1.6 m/z and fragmented by higher energy collision-induced dissociation (HCD) with 35% of collision energy. The resulting fragments were detected by the linear ion trap in rapid scan rate with an AGC target of $1 \times 10^4$ and a maximum injection time of 50 ms. Dynamic exclusion of previously fragmented peptides was set for a period of 20 s and a tolerance of 10 ppm.

The results were obtained and analyzed using Scaffold Protein software. The list of identified proteins was filtered using a protein threshold of 99%, a peptide threshold of 95%, and a minimum of 1 peptide identified in each sample. Proteins interacting with the control RNA sequence were excluded, and only proteins that specifically interacted with the ncRNA97 sequence in triplicate samples were included in the results. The details of the mass spectrometry and database search protocols and criteria for protein identification have been described elsewhere (Lorenzon et al., 2022).

## 2.10 Phenotypical assays

To evaluate the nutritional stress response of promastigotes in the log phase, parasites at $10^6$ cells·mL$^{-1}$ were incubated for 2 or 4 h in PBS for total starvation. Subsequently, the cells were pelleted and resuspended in 100 µL fresh M199 medium and seeded in a 96-well plate for 20 h at 27°C for recovery. Then, 10 µL of 1 mg·mL$^{-1}$ MTT was added to each well, and the plate was incubated for another 4 h. Afterward, the plate was centrifuged at 2,000 × g, and the pellet was resuspended in 100 µL of DMSO, after which the absorbance was measured at 570 nm. Non-starved cells were used as a negative control and were considered to have 100% cell viability. For oxidative stress response assays, $10^6$ cells·mL$^{-1}$ axenic amastigotes were incubated for 24 h in FBS containing 300 µM $H_2O_2$ at 33°C in a 5% $CO_2$ atmosphere. After treatment, the cells were pelleted, resuspended in 100 µL fresh FBS, and then seeded in a 96-well plate for the same viability assay as described for nutritional stress. For metacyclogenesis rate, promastigotes were culture until the stationary phase and pelleted by centrifugation at 2,000 × g 10min. Then, metacyclic form was collected through a Ficoll gradient, as previous described (Späth and Beverley, 2001). Total cells before the fractionation was considered as 100% of alive cells and the amount of cells collected after the Ficoll gradient was used to estimate the percentage of cell differentiation.

## 2.11 Statistical analysis

The experiments were performed in biological triplicates, and statistical analyses (ANOVA with Dunnett's test) were performed using GraphPad Prism 8. $p<0.05$ was considered to indicate statistical significance. Statistically significant differences are indicated by asterisks, where $^{**}p \leq 0.002$, $^{***}p \leq 0.0002$ and $^{****}p \leq 0.0001$.

# 3 Results

## 3.1 Confirmation, differential expression and processing feature analysis of ncRNA97

To identify small ncRNAs for functional investigation, we focused on those reported by Ruy et al. (2019). as differentially expressed. A manual inspection was performed to select ncRNAs smaller than 200 nucleotides, considering parameters such as proximity to coding sequences (CDSs), transcriptional orientation (same as the corresponding PTU), and sequence quality for designing donor and guide RNAs.

We initially selected eight putative ncRNAs that were preferentially expressed in metacyclic or amastigote stages (Figure 1A). Knockouts were successfully generated for five of them, and all were tested for their impact on promastigote growth patterns. Each knockout exhibited varying levels of commitment to promastigote multiplication (Figures 1B, C). Among these, LbrM2903_20.1_ncRNA97 (hereafter referred to as ncRNA97) showed the most significant effect and was selected for further investigation.

RNA-seq predicted ncRNA97 to be a 148-nucleotide-long transcript (Figure 1A) preferentially expressed in amastigotes (Ruy et al., 2019). It is located on chromosome 20, and it has been annotated as an independent transcript between two protein-encoding genes (Figure 1A). Nevertheless, the lack of a clear gap in RNA read density between the upstream transcript and the ncRNA97 sequence suggests that ncRNA97 could also be within the 3'UTR of the upstream transcript (Figure 1A). Therefore, we confirmed the differential expression of ncRNA97 by RT–qPCR (Figure 1B) and determined its size and the nature of its 3′ and 5′ ends by a circular RNA assay (Hang et al., 2015). Briefly, total RNA was treated (or not treated) with tobacco acid pyrophosphatase (TAP) to generate 5′-monophosphate RNAs of transcripts bearing a cap to allow circularization after RNA ligase addition. From this circular RNA, cDNA was generated, and primers specific to the ncRNA97 sequence were used, which were directed outward of the transcript in each extremity. Different PCR products were identified (Supplementary Figure 2D), and three bands of approximately 150, 500 and 600 nucleotides were sensitive to TAP and likely to be capped or triphosphorylated RNA (Figure 1C). The TAP-sensitive amplicon of 500 nucleotides and seven other PCR products, ranging from 177 to 838 nucleotides, were sequenced, and the predicted ncRNA97 sequence was confirmed in all of them. The poly(A) tail length varied from 0 ≈ 64 nucleotides (Figure 1D; Supplementary Figure 2E). Notably, no ME was detected in any sequence, even in the TAP-dependent PCR product (band F.3 in Supplementary Figure 2E). This was unexpected, as the 5′ cap of trypanosomatid mRNAs is added via the capped ME sequence in the trans-splicing reaction. To further confirm the protection at the 5' end of this transcript, total RNA was treated or not treated with mRNA decapping enzyme (MDE) plus 5'→3' XRN-1 exoribonuclease to degrade 5'-monophosphate RNA. Afterward, the remaining RNA was reverse-transcribed to DNA, and ncRNA97 was amplified by PCR. Amastin (LBRM2903_080014000) and rRNA45 transcripts were used as coding and noncoding controls, respectively. PCR products were obtained for all transcripts, independent of the treatment (MDE or XRN-1) (Figure 1E), suggesting 5' protection of these RNAs. After MDE and XRN-1 treatments, rRNA45 and amastin transcripts were barely detected, while ncRNA97 was very evident. Together, these results indicate that ncRNA97 is not a 5′-monophosphorylated RNA but is protected at its 5′ end in a way that is distinct from the traditional CAP found in *Leishmania* coding genes. Additionally, secondary structure in six of the seven ncRNA97 isoforms detected by the circularization assay was predicted to be an elongated hairpin with two large and one

10.3389/fcimb.2025.1513908

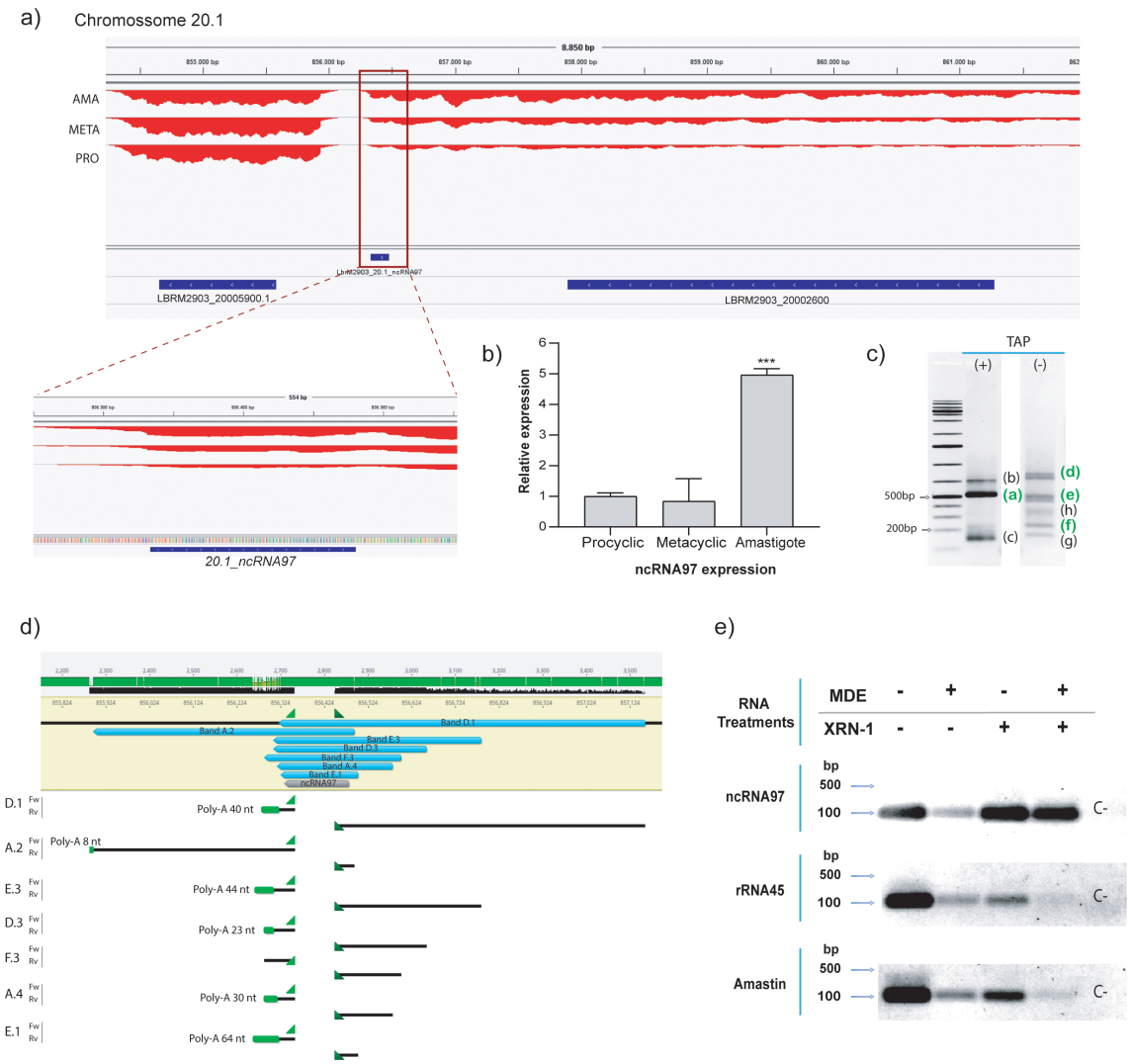


FIGURE 1
General overview and processing of ncRNA97. **(A)** Genomic location of ncRNA97 in an intergenic region on chromosome 20.1. **(B)** Confirmation of differential expression of ncRNA97 in axenic amastigotes compared to procyclic and metacyclic amastigotes by RT–qPCR. **(C)** RNA circularization assay with or without TAP treatment (see SF1A for methods) and detection of amplified transcript ends by conventional PCR. Bands identified in green were successfully cloned and sequenced. **(D)** Sequencing revealed different lengths for ncRNA97 transcripts in the cell, with the predicted sequence identified in all transcripts. Poly-A tails are indicated in green. No mini-exon was detected in any of the sequenced ncRNA97 transcripts. **(E)** Total RNA samples were treated (+) or not (-) with mRNA decapping enzyme (MDE) for cap removal and/or with XRN-1 5′→3′ exonuclease for 5′-monophosphate RNA degradation. Then, the RNA was recovered by chloroform extraction and ethanol precipitation, which was followed by reverse transcription and conventional PCR to detect conventionally 5′ capped transcripts. Amastin (LBRM2903_080014000) and rRNA45 transcripts were used as coding and noncoding RNA controls, respectively. A negative control (C-) was generated via PCR with no DNA input.

smaller loop (Supplementary Figure 3), which might be relevant for the function or stability of the ncRNA97.

## 3.2 ncRNA97 functions: cis- and trans-regulation of gene expression

ncRNA97 knockout ($^{KO}$) parasites were generated in the *L. braziliensis* M2903 strain via CRISPR/Cas9 genome editing (Beneke et al., 2017), and homozygote parasites were confirmed by conventional PCR and total RNA-seq analysis (Supplementary Figures 4B, C). The genomic position of the primers used for the replacement of ncRNA97 with a selectable marker, the sequence of the guide and donor, and the confirmation of the replacement are shown in Supplementary Figures 3A, 3B. The ncRNA97 knockout negatively affected the transcript levels of the gene upstream (UP) of ncRNA97 (LBRM2903_200026000 – FtsX-like protein), whereas the transcript level of the downstream (DW) gene (LBRM2903_200025900 – hypothetical protein) was not affected (Figure 2A). The localization of the FtsX-like transcript was not altered in ncRNA97$^{KO}$ cells (Figure 2B), indicating that ncRNA97 does not function in regulating nuclear export or cytoplasmic

10.3389/fcimb.2025.1513908

stability. Add-back (ncRNA97$^{AB}$) parasites were generated by transfecting the ncRNA97$^{KO}$ cell line with a plasmid encoding the ncRNA97 sequence predicted by RNA-seq (Supplementary Figure 5). RT–qPCR confirmed that the expression of ncRNA97 in the add-back cells was ~3 times greater than that in the parental cells (Figure 2C). Importantly, the levels of the downregulated FtsX-like gene fully recovered to the levels in the parental cells (Figure 2C). The rescue of FtsX transcript levels by ectopic ncRNA97 expression indicates a trans-regulatory function for ncRNA97, albeit emerging from its (potential) target, suggesting that it may act as a *cis*-ncRNA.

Next, to investigate the possible *trans*-regulatory function of ncRNA97, the transcriptome of the parental cells was compared with that of ncRNA97$^{KO}$ parasites (Figure 2D). A relatively small number of genes were upregulated (8) or downregulated (37) (Supplementary Figure 6), among which the top 4/5 (up/down) with the highest fold change (FC) were considered for further investigation. The transcript levels of the putative core histones

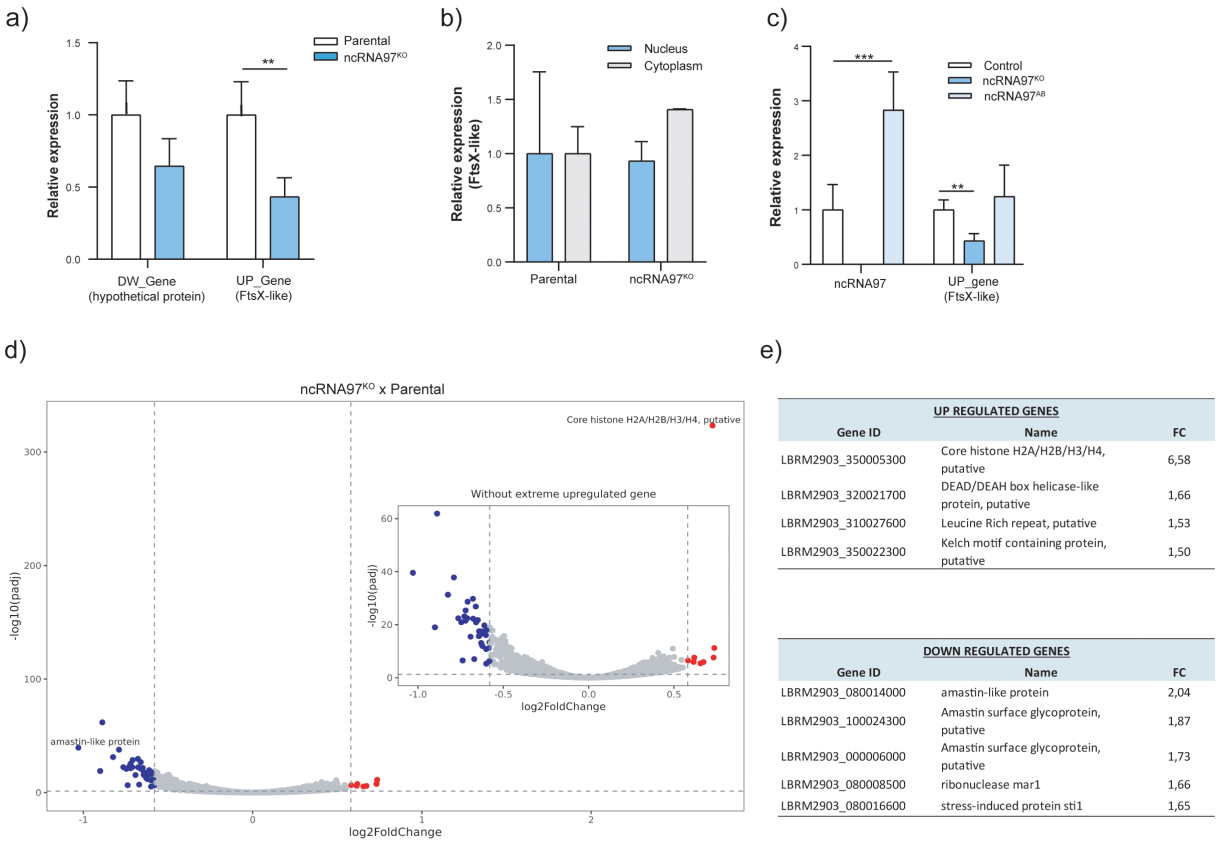


**UP REGULATED GENES**

| Gene ID | Name | FC |
|---|---|---|
| LBRM2903_350005300 | Core histone H2A/H2B/H3/H4, putative | 6,58 |
| LBRM2903_320021700 | DEAD/DEAH box helicase-like protein, putative | 1,66 |
| LBRM2903_310027600 | Leucine Rich repeat, putative | 1,53 |
| LBRM2903_350022300 | Kelch motif containing protein, putative | 1,50 |

**DOWN REGULATED GENES**

| Gene ID | Name | FC |
|---|---|---|
| LBRM2903_080014000 | amastin-like protein | 2,04 |
| LBRM2903_100024300 | Amastin surface glycoprotein, putative | 1,87 |
| LBRM2903_000006000 | Amastin surface glycoprotein, putative | 1,73 |
| LBRM2903_080008500 | ribonuclease mar1 | 1,66 |
| LBRM2903_080016600 | stress-induced protein sti1 | 1,65 |

FIGURE 2
Epigenetic alterations in ncRNA97$^{KO}$ parasites. **(A)** Downregulation of the upstream gene LBRM2903_20002600 (FtsX-like) in the ncRNA97$^{KO}$ parasites was observed by RT-qPCR. **(B)** Intracellular location of the FtsX-like transcript in the parental and ncRNA97$^{KO}$ parasites were compared. **(C)** The expression level of the upstream gene in ncRNA97$^{AB}$ parasites. **(D)** Volcano plot showing genes with differential expression between ncRNA97$^{KO}$ and parental cells. **(E)** The top 4 and 5 genes identified as differentially expressed in the ncRNA97$^{KO}$ cells based on their p values for up- and downregulated genes, respectively. **(F)** The levels of upregulated and **(G)** downregulated genes levels were restored to near-parental levels in ncRNA97$^{AB}$ parasites. 7SL and G6PD transcripts were used as housekeeping genes to normalize the data.

10.3389/fcimb.2025.1513908

H2A/H2B/H3/H4 and DEAD/DEAH box helicase were 6.6 and 1.7 times greater, respectively, in the ncRNA97$^{KO}$ cells than in the parental cells (Figure 2E). Interestingly, three out of the five downregulated transcripts encoded amastin, with FCs between 2.0 and 1.7, while the other two encoded the ribonuclease mar1 and stress-induced protein 1 (STI1) (Figure 2E). Amastin, a multigene family with most isoforms exclusively or preferentially expressed in amastigotes, is crucial for the intracellular viability of *L. braziliensis* amastigotes (de Paiva et al., 2015). Notably, these three downregulated transcripts encode different amastin isoforms with divergent peptide sequences (Supplementary Figure 7). To confirm the RNA-seq results, RT–qPCR was performed for two up- and downregulated genes. Significant differences between the ncRNA97$^{KO}$ and ncRNA97$^{AB}$ cells were observed for the two upregulated genes, in agreement with the RNA-seq data, but not for the downregulated genes (Figures 2F, G, respectively). Importantly, the RT–qPCR assays were performed in promastigotes, and the low transcript levels of amastin (LBRM2903_080014000) in this stage may have impaired the evaluation of differences, as indicated by the ΔCT values of the RT–qPCR analysis (Supplementary Figure 4E). However, in ncRNA97$^{KO}$, the ΔCT values were greater than 37, indicating that this gene is expressed at very low levels in ncRNA97$^{KO}$ parasites. Thus, considering their ΔCT values, we may assume that the expression levels of these genes recovered to the parental level in the add-back parasites (Supplementary Figure 4E). These results suggest a correlation between the levels of ncRNA97 and the abundance of certain protein-coding transcripts.

## 3.3 ncRNA97 protein partners and putative functions

Knowing that ncRNA functions might depend on their intracellular localization and association with proteins (Junge et al., 2017), after total RNA fractionation, we quantified the intracellular location of ncRNA97 by RT–qPCR using GAPDH as endogenous control. Interesting, predominant nuclear localization (>99%) for ncRNA97 was observed in procyclic promastigotes in the parasite log phase growth (Figure 3A). Considering that regulatory ncRNAs might function as part of macromolecular complexes, we searched for protein binding partners of ncRNA97 by pulldown *in vitro* assays and mass spectrometry. Statistical analysis ($p$<0.05) revealed 63 proteins enriched for interactions with ncRNA97 relative to the aptamer only (Figure 3B; Supplementary Figure 8B). Of these, 25 had predicted functions and were subjected to Gene Ontology (GO) analysis to identify potential processes in which ncRNA97 could be involved (Tang et al., 2023).

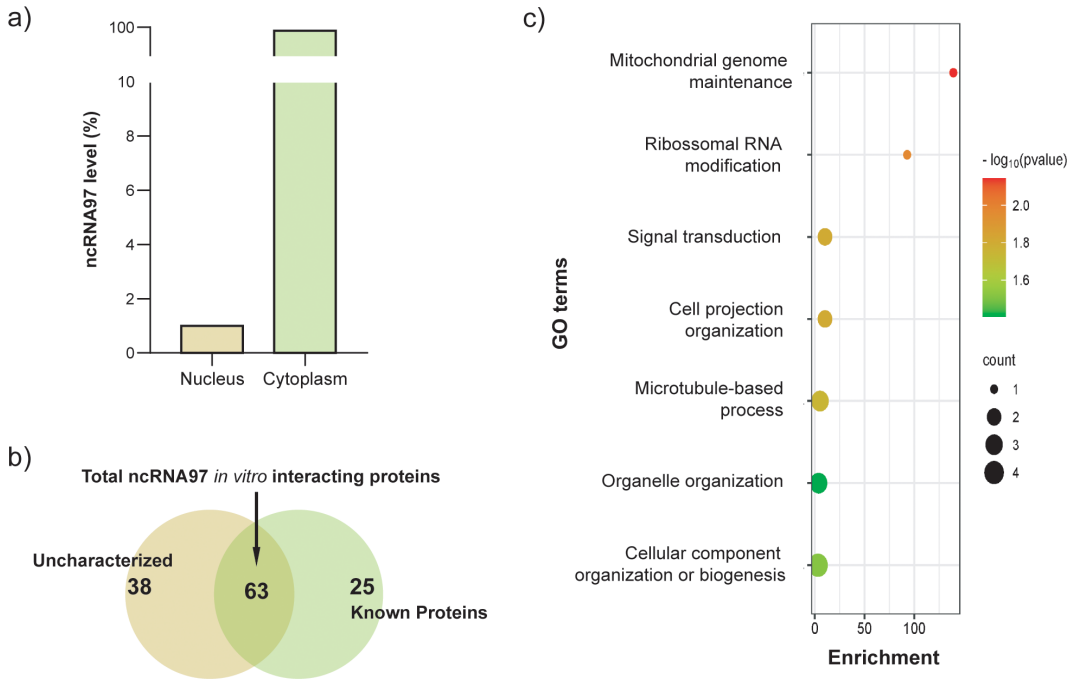


FIGURE 3
Intracellular localization of ncRNA97 and its respective interacting proteins. **(A)** Total RNA from promastigotes in the log phase was fractionated, and the relative expression of ncRNA97 was estimated by RT–qPCR; the standard deviation was lower than 5%. **(B)** Proteins found as specifically bound to the ncRNA97 predicted sequence through an *in vitro* pulldown assay,. **(C)** After statistical analysis using a t test and considering a p value <0.05, the 63 proteins identified as specifically binding to the ncRNA97 sequence by *in vitro* pulldown assay were subjected to GO analysis. See the supplemental material for the complete list.

10.3389/fcimb.2025.1513908

Interestingly, one of the identified proteins was a putative rRNA methyltransferase protein (A4HFX5_LEIBR) related to rRNA modification according to its GO annotations (Figure 3C; Supplementary Figure 8B). This protein is homologous to Spb1 from *Trypanosoma brucei*, a protein that is involved in rRNA methylation and processing and relevant to ribosome assembly (Liang et al., 2005). Remarkably, the ribosomal protein L31, a large ribosomal subunit constituent (Liu et al., 2016) and a eukaryotic translation factor were detected among the ncRNA97 partners in the pulldown assays. The pulldown results led us to hypothesize that ncRNA97 might play a role in ribosomal processing/assembly.

## 3.4 ncRNA97 affects growth, metacyclogenesis, and the nutritional stress response

ncRNA97$^{KO}$ parasites were then screened for phenotypic alterations relative to the parental cell line (Supplementary Figure 4F). Compared with control cells, cultured ncRNA97$^{KO}$ cells had a longer doubling time (Supplementary Figure 4G). This growth phenotype was not caused by the downregulation of the FtsX-like transcript, the ncRNA97-upstream gene, as FtsX-like $^{KO}$ cells grew normally (Figure 2C; Supplementary Figure 4G). The increased doubling time of the ncRNA97$^{KO}$ cells may partially explain their poorer metacyclogenesis rate, which was indicated by the results of the metacyclic enrichment Ficoll assay (Späth and Beverley, 2001) (Figure 4A). Additionally, MTT colorimetric assays to evaluate promastigote viability after starvation in PBS for 4 h indicated that ncRNA97 $^{KO}$ parasites were more sensitive to nutritional stress than the parental and FtsX-like $^{KO}$ parasites (Figure 4B). Moreover, after 4 h of starvation, the ncRNA97 levels in the parental cells decreased significantly, with partial recovery after 24 h of incubation in fresh medium (Figure 4C). Axenic amastigotes were evaluated for oxidative stress response, and despite the lower resistance of ncRNA97 $^{KO}$ axenic amastigotes (Supplementary Figure 3H) to $H_2O_2$, the parasite infectivity in THP-1 macrophages and intracellular proliferation *in vitro* were similar to those in the parental cells (Supplementary Figures 4I, J). The metacyclogenesis rate recovered to the parental level in ncRNA97$^{AB}$ parasites, suggesting that ncRNA97 impairs metacyclogenesis in ncRNA97$^{KO}$ parasites (Figure 4D).

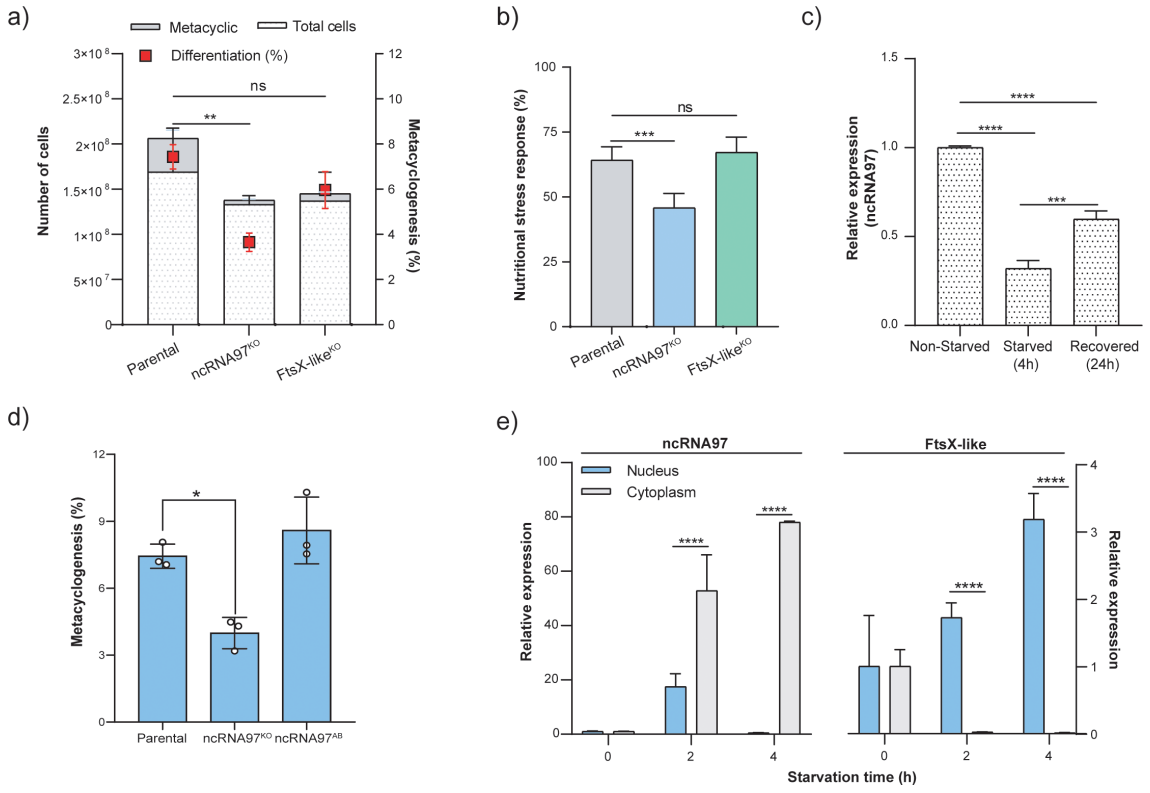


FIGURE 4
Phenotypic alterations in ncRNA97$^{KO}$ cells and ncRNA97 cell distribution and intracellular localization during starvation. **(A)** The percentage of the metacyclic form in the stationary phase was used to estimate the metacyclogenesis rate by a Ficoll density gradient assay (Späth and Beverley, 2001). **(B)** MTT viability assay showing the sensitivity of parasites lacking ncRNA97 to 4 h of nutritional stress in PBS. **(C)** Transcript level of ncRNA97 for parasites after 24 h of recovery after starvation was determined by RT–qPCR. Quantification is relative to the expression levels of the endogenous transcript (G6PDH). **(D)** Metacyclogenesis rate in ncRNA97$^{AB}$ parasites compared to parental cell line. **(E)** Cytoplasmic accumulation of ncRNA97 transcripts increased in a starvation time-dependent manner and was not correlated with the localization of the upstream transcript LBRM2903_20002600, which accumulated in the nucleus.

Next, we evaluated the intracellular distribution of ncRNA97 via subcellular fractionation and subsequent quantification of the nuclear and cytoplasmic levels of ncRNA97 under normal and starvation conditions by RT–qPCR. Interestingly, both the subcellular distribution and levels of ncRNA97 changed with nutritional stress. The cytoplasmic accumulation of ncRNA97 transcripts increased with starvation time to approximately 80-fold after 4 h of starvation in PBS and was barely detectable in the nucleus under these conditions (Figure 4E). Notably, the observed dynamics of ncRNA97 expression and localization are markedly distinct from those of its upstream gene, since the FtsX-like transcript accumulated in the nucleus after nutritional stress (Figure 4E). Additionally, no difference in the nuclear or cytoplasmic levels of FtsX-like transcripts was detected between the parental and ncRNA97$^{KO}$ cells (Figure 2B).

## 4 Discussion

Regulatory ncRNAs have been identified in various organisms, where they play diverse physiological and pathological roles, though their mechanisms of action are often poorly understood. In the protozoan parasite *Leishmania*, research is beginning to uncover the presence of regulatory ncRNAs and their potential functional roles (Iribar et al., 2003; Freitas Castro et al., 2017; Ruy et al., 2019). In this study we demonstrated that ncRNA97, a small ncRNA preferentially expressed in amastigotes—the proliferative stage within the host—is involved in gene expression regulation and influences metacyclogenesis as well as the parasite's response to nutritional stress. While this targeted approach yields valuable insights, it highlights the limitations of studying ncRNAs individually when aiming to understand their broader roles in the parasite. High-throughput reverse genetics assays are indispensable for systematically and efficiently exploring the roles of ncRNAs in parasite development or host-parasite interacion, following approaches utilized for mRNAs (Aellig et al., 2024). Our findings underscore that the exploration of ncRNAs is still in its early stages, with much to discover about their roles in regulating biological processes and mechanisms critical for cellular homeostasis and development in pathogenic eukaryotes. The scarcity of research on regulatory ncRNAs in *Leishmania* and similar pathogens can be attributed to challenges such as technical limitations, the lack of conserved primary sequences in functional transcripts, and diverse modes of action. Addressing these challenges is pivotal to advancing our understanding of these crucial regulatory molecules.

Nevertheless, a target approach is quite valuable and herein we confirmed the presence, differential expression, length, and processing of the ncRNA97 predicted based on RNA-seq data (Ruy et al., 2019). We have witnessed a putative length polymorphism of the transcript as revealed via an RNA circularization assay. For the seven sequenced ncRNA97 transcripts, we have no data on the preferential isoform or whether they vary depending on the stage or are generated on subsequent processing and cleavages, but all of them present a conserved primary predicted sequence, with six of seven with conserved secondary structure. Considering that apart from mRNAs, all the other classes of RNAs depend primarily on the secondary structure to be functional, we might hypothesize that the observed structure is central to the interaction of ncRNA97 with partner proteins and consequently to its functions, but this hypothesis must be investigated for confirmation.

The RNA circularization assay, combined with treatments using an mRNA decapping enzyme (MDE) and a 5'→3' exonuclease (XRN-1), revealed that most of the sequenced transcripts are polyadenylated. Additionally, the 5' end of ncRNA97 is protected, but the transcript is neither a product of the typical trypanosomatid *trans*-splicing process (Lebowitz et al., 1993) nor a 5'-monophosphorylated RNA.

We might speculate that ncRNA97 carries an alternative cap structure at its 5' end. Of note, as a result of awareness and with the increased sensitivity of RNA sequencing and small-molecule mass spectrometry, the last decade has been marked by an increment of known chemical modifications on mRNAs (Gilbert et al., 2016). It is known that 5′ nicotinamide-adenine dinucleotide (NAD+) RNA, previously shown in bacteria, exists in *Saccharomyces cerevisiae*, and 5′ NAD-RNA has been demonstrated on subsets of nuclear and mitochondrial encoded mRNAs (Walters et al., 2017). Also, N6-methyladenosine within the 5′UTR of an mRNA are translated in a cap-independent manner (Meyer et al., 2015) and it has been shown that the biogenesis of uncapped mRNA isoforms, which are numerous in the human transcriptome, may involve alternative endonuclease cleavage and polyadenylation (Malka et al., 2022). These and other alternative processing of coding and non-coding transcripts must be investigated to understand the biogenesis and the structure present at the 5'termini of the ncRNAs in *Leishmania* such as ncRNA97.

In future studies, the possible role of endoribonucleases in the cleavage that generates these ncRNAs should be investigated, as this process has been observed in ncRNAs from mammalian cells (Mercer et al., 2011; Luciano and Belasco, 2019). We have not conducted any assay to confirm that the upstream gene and ncRNA97 are generated as a single transcript and that cleavage to release ncRNA97. However, the transcriptome profile obtained showed no clear difference in the number of reads between the ncRNAs and the upstream mRNAs, supporting this hypothesis.

With no prior information about the potential roles of the studied DE ncRNA, we generated ncRNA97$^{KO}$ parasites to investigate the possible functional effects of ncRNA97. In this context, we reintroduced the transcript sequence predicted by RNA-seq using plasmid expression to create ncRNA97$^{AB}$ cells. This approach allowed us to confirm which knockout phenotypes were reverted upon reintroduction of the gene. and a knockout of

the ncRNA97 upstream gene, FtsX-like, was used to ensure those phenotypic changes were due to ncRNA97 knockout. These cell lines were analyzed for several properties, such as growth under axenic conditions to evaluate phenotypic alterations in promastigote doubling time, *in vitro* infectivity, and metacyclogenesis, as well as for response to nutritional and oxidative stresses, conditions mimicking some of the hostile environments encountered during the parasite lifecycle. ncRNA97$^{KO}$ parasites displayed a longer promastigote doubling time and impaired metacyclogenesis compared to parental and FtsX-like$^{KO}$ lines, indicating a specific role for ncRNA97. Their response to starvation also differed significantly from parental cells, likely due to slower growth and reduced differentiation. Despite these defects, ncRNA97$^{KO}$ intracellular amastigote replication was similar to that of parental cells *in vitro*.

Notably, ncRNA97$^{KO}$ parasites showed increased sensitivity to oxidative stress recovery (24 h in H2O2), a key challenge for amastigotes within macrophages (da Silva et al., 2017). These findings suggest that ncRNA97 influences parasite duplication and modulates responses to nutritional stress and differentiation, processes crucial for parasite survival and adaptation.

One possible role for ncRNAs is the modulation of the levels of neighboring genes; these transcripts are retained at the chromatin of the locus of origin as *cis*-regulatory ncRNAs (Bumgarner et al., 2009; Engreitz et al., 2016; Gil and Ulitsky, 2020). Therefore, we examined the levels of the up- and the downstream genes and the downregulation of the upstream gene (FtsX-like) was observed in the ncRNA97$^{KO}$ parasites, FtsX-like transcript levels were recovered to the parental levels in ncRNA97$^{AB}$ cells, indicating a positive correlation between the levels of this transcript and the presence of ncRNA97 in the cells. The subcellular localization of the FtsX-like transcript was not affected by the presence or absence of ncRNA97, despite the effects on upstream gene levels. It could be argued that this effect may result from the role of the 3'UTR cis-element rather than ncRNA97 functioning as an independent transcript. As well-established, 3'UTR elements often act as binding sites for proteins that regulate mRNA stability, abundance, or translation efficiency (Yamashita and Takeuchi, 2017). However, the ectopic add-back system used suggests that ncRNA97 behaves as an individual regulatory ncRNA, directly acting on its original locus, and not as a 3'UTR element of the upstream gene.

It is well established in other organisms that ncRNAs might act as regulators at different levels, including through modulation of the stability or translation rate of their target mRNAs (Huang et al., 2022). In fact the comparative transcriptomic analysis revealed that ncRNA97 also acts at the transcriptional level to modulate genes from different loci, suggesting a *trans*-regulatory activity. Indeed, several transcripts were found to be up- or downregulated in ncRNA97$^{KO}$ parasites, including the core histone gene and some genes encoding amastin, an amastigote-specific protein (Wu et al., 2000; Rochette et al., 2005). Additionally, the gene encoding the stress-induced STI1 protein was downregulated in the ncRNA97$^{KO}$ cells, what must be further investigated to confirm a possible link to ncRNA97$^{KO}$ parasites lower nutritional stress resistance. This protein was characterized in promastigotes from *L. major* as a heat stress response-dependent protein, in addition to complexing with Hsp70 and Hsp83 chaperones in other organisms (Webb et al., 1997). Additionally, STI1 is present at higher levels in epimastigotes from *T. cruzi* under nutritional stress, and impaired differentiation was observed in the STI1$^{KO}$ parasite (Schmidt et al., 2018). Similarly, stress response and metacyclogenesis phenotypes were observed for *L. braziliensis* ncRNA97$^{KO}$ promastigotes. Consistently, the levels of these up- and downregulated genes recovered to the parental levels in ncRNA97$^{AB}$ parasites, confirming the correlation between the levels of these genes and ncRNA97. Overall, the phenotypic and transcriptomic results corroborate the involvement of ncRNA97 at different stages of *Leishmania* development.

Modulation of the stability or translation rate of their target mRNAs might be mediated through ncRNA-protein complexes, like observed in *T. brucei*, which these interactions were confirmed for *Grumpy*, a ncRNA involved in parasite differentiation (Guegan et al., 2022). Thus, we conducted an *in vitro* assay to identify proteins that specifically bind to the ncRNA97 sequence. Among the 25 proteins identified with a p value <0.05 that also had a predicted function, we identified a putative rRNA methyltransferase protein (LbrM.27.2160). This methyltransferase protein is the sole protein identified to be involved in the rRNA modification pathway, which is poorly characterized in trypanosomatids. The rRNA methyltransferase protein is a nucleus-preferential protein involved in rRNA maturation and the biogenesis of ribosomal subunits in other eukaryotes (Satterwhite and Mansfield, 2022). ncRNA97 was primarily detected in the nuclei of promastigotes in the log phase of growth, under physiological conditions, which supports the hypothesis that it may interact with these macromolecules *in vivo* and might be involved in rRNA processing, what requires further investigation.

In *T. brucei*, it was reported that an abundant tRNA-derived ncRNA is produced under starvation conditions and is involved in facilitating the recovery of mRNA loading to normal levels once starvation is halted (Fricker et al., 2019). In *L. braziliensis*, despite the decrease in total ncRNA97 under nutritional stress conditions, a starvation time-dependent increase in cytoplasmic ncRNA97 (~80 times) was observed. Thus, we may assume that starvation does not trigger an increment of ncRNA97 transcript levels, as observed for the tRNA fragment in *T. brucei* (Fricker et al., 2019), but that its subcellular localization is altered under this environmental condition.

Despite ncRNA97 predominant nuclear localization under physiological conditions, the pulldown assay showed several ncRNA97 interacting proteins indicating ncRNA97 might play a role and should be localized in the cytoplasm. Among these proteins, the ribosomal protein (RP) L31 and the translational

10.3389/fcimb.2025.1513908

initiation factor 2 (eIF2α) were identified. Of note, in *Leishmania*, the level of eIF2α is directly associated with the protein synthesis rate (Lahav et al., 2011), and eIF2α phosphorylation is essential for parasite survival under stress conditions (Abhishek et al., 2017), which is consistent with the poorer response of ncRNA97$^{KO}$ parasites to nutritional stress. Interestingly, under nutritional stress ncRNA97 switches location and is predominantly found in the cytoplasm. In mammalian cells, aberrant expression of L31 ribosomal protein has been associated with cancer malignancy, affecting signaling pathways (Wu et al., 2023), but in trypanosomes, RPL31, apart from a structural component of the large ribosomal subunit is associated with a small rRNA (srRNA3) involved in the process of ribosome assembly (Liu et al., 2016). Thus, the interactions of ncRNA97 with L31 and with a protein involved in rRNA methylation (LbrM.27.2160), predicted in the *in vitro* pulldown assay, should be investigated to evaluate a putative relevance of ncRNA97 for ribosome functionality. In fact, ncRNA97 is preferentially expressed in amastigotes and seems to regulate the levels of amastigote-specific genes. However, the observed phenotypes indicate that the function of ncRNA97 does not depend on its level in the cell, since most of the alterations were observed in the promastigotes, such as a decrease in the nutritional stress response and differentiation rate.

Ultimately, our results support the hypothesis that functions for ncRNA97 occurs at both *cis*- and *trans*-regulatory levels, coordinating the modulation of the levels of some coding genes and phenotypic alterations (Figure 5). As shown for a group transcripts, they are directly affected on their levels depending on the presence or absence of ncRNA97. ncRNAs in other organisms have been shown to play regulatory *cis*- and *trans*- functions, such as lncRNA Jpx, a ncRNA that coordinates Xist gene products *in vivo* (Carmona et al., 2018). Clearly, further investigation is required to fully understand and elucidate the mechanism of action of ncRNA97 and the relevance of its secondary structure. Finally, the results herein present the first robust molecular and functional characterization of a short ncRNA in *L. braziliensis*. Other differentially expressed ncRNAs in these parasites may also play relevant roles in the protozoan development, and investigating them could provide insights into ncRNAs as targets for therapeutic options in the future.

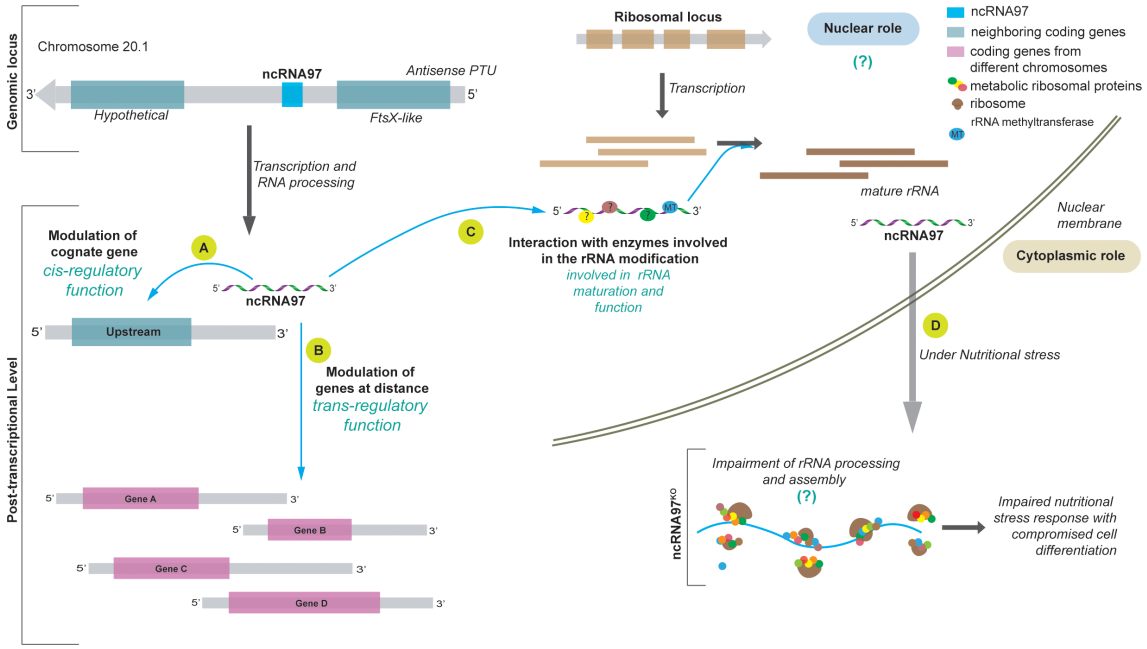


FIGURE 5
Model of the ncRNA97 levels of action in *L. braziliensis*. **(A)** After transcription, ncRNA97 acts as a *cis*-regulatory ncRNA regulating the FtsX-like transcript level. **(B)** ncRNA97 may also act as a *trans*-element regulating the levels of a group of mRNAs from different genomic loci by an unknown mechanism. Such interactions probably occur in RNP complexes that include RNA binding proteins (?). **(C)** Still in the nucleus, ncRNAs seem to interact with proteins involved in ribosomal (r) RNA processing, such as rRNA methyltransferase protein (MT), to generate mature rRNAs. **(D)** In the cytoplasm, under nutritional stress, the ncRNA97$^{KO}$ parasites are less resistant and exhibit a lower differentiation rate, probably due to incorrect rRNA processing. In control cells, ncRNA accumulates in the PP fraction under nutritional stress ().

## Data availability statement

The datasets presented in this study can be found in online repositories. The names of the repository/repositories and accession number(s) can be found in the article/Supplementary Material.

## Author contributions

JQ: Data curation, Formal analysis, Investigation, Methodology, Writing – original draft, Writing – review & editing. CE: Investigation, Methodology, Writing – review & editing. LO: Data curation, Formal analysis, Investigation, Writing – review & editing. TD: Methodology, Writing – review & editing. LA: Methodology, Writing – review & editing. FH: Formal analysis, Investigation, Methodology, Writing – review & editing. AC: Conceptualization, Formal analysis, Funding acquisition, Resources, Supervision, Writing – review & editing.

## Funding

The author(s) declare financial support was received for the research, authorship, and/or publication of this article. This project was supported by Fundação de Amparo à Pesquisa do Estado de São Paulo, FAPESP (https://fapesp.br/en) (2018/14398-0, 2015/13618-8, grants to AC); the Brazilian National Council for Scientific and Technological Development (https://www.gov.br/cnpq/pt-br), CNPq (305775/2013-8 and 152584/2022-6) to AC and LA. This study was also supported in part by the Coordenação de Aperfeiçoamento de Pessoal de Nível Superior -Brazil (CAPES, https://www.gov.br/capes/pt-br), Finance Code 001, to AC. JQ (2020/00088-9), CE (2020/00087-2), LA (2017/19040-3) and LO (2021/10043-5) were supported by FAPESP fellowships. The funders had no role in the study design, data collection and analysis, decision to publish, or preparation of the manuscript.

## Acknowledgments

We would like to thank Dr Susanne Kramer from the University of Würzburg, Germany, for the critical discussions that improved the work and for opening her laboratory and resources for training for JQ; Viviane Ambrósio for the technical support in the laboratory; Dr Gustavo D. Campagnaro for sharing tools; Dr Pegine Walrad from the University of York for materials exchanges; and the staff of the Proteomics Platform of the CHU de Québec Research Centre, Québec, Canada. We also acknowledge TriTrypDB for providing indispensable resources and tools.

## Conflict of interest

The authors declare that the research was conducted in the absence of any commercial or financial relationships that could be construed as a potential conflict of interest.

## Generative AI statement

The author(s) declare that no Generative AI was used in the creation of this manuscript.

## Publisher's note



## Supplementary material

The Supplementary Material for this article can be found online at: https://www.frontiersin.org/articles/10.3389/fcimb.2025.1513908/full#supplementary-material

## References

Abhishek, K., Sardar, A. H., Das, S., Kumar, A., Ghosh, A. K., Singh, R., et al. (2017). Phosphorylation of Translation Initiation 2-Alpha in Leishmania donovani under stress is necessary for Parasite Survival. *Mol. Cell. Biol.* 37, 1–19. doi: 10.1128/MCB.00344-16

Aellig, S., Billington, K., Damasceno, J. D., Davidson, L., Dobramysl, U., Etzensperger, R., et al. (2024). LeishGEM: genome-wide deletion mutant fitness and protein localisations in Leishmania. *Trends Parasitol.* 40, 675–678. doi: 10.1016/j.pt.2024.06.003

Bates, P. A. (2007). Transmission of Leishmania metacyclic promastigotes by phlebotomine sand flies. *Int. J. Parasitol.* 37, 1097–1106. doi: 10.1016/j.ijpara.2007.04.003

Batugedara, G., Lu, X. M., Hristov, B., Abel, S., Chahine, Z., Hollin, T., et al. (2023). Novel insights into the role of long non-coding RNA in the human malaria parasite, Plasmodium falciparum. *Nat. Commun.* 14, 1–19. doi: 10.1038/s41467-023-40883-w

Beneke, T., Madden, R., Makin, L., Valli, J., Sunter, J., and Gluenz, E. (2017). A CRISPR Cas9 high-throughput genome editing toolkit for kinetoplastids Subject Category: Subject Areas. *R. Soc Open Sci.* 4, 170095. doi: 10.1098/rsos.170095

Brannan, C. I., Dees, E. C., Ingram, R. S., and Tilghman, S. M. (1990). The product of the H19 gene may function as an RNA. *Mol. Cell. Biol.* 10, 28–36. doi: 10.1128/mcb.10.1.28-36.1990

Bumgarner, S. L., Dowell, R. D., Grisafi, P., Gifford, D. K., and Fink, G. R. (2009). Toggle involving cis-interfering noncoding RNAs controls variegated gene expression in yeast. *Proc. Natl. Acad. Sci. U. S. A.* 106, 18321–18326. doi: 10.1073/pnas.0909641106

Carmona, S., Lin, B., Chou, T., Arroyo, K., and Sun, S. (2018). LncRNA Jpx induces Xist expression in mice using both trans and cis mechanisms. *PloS Genet.* 14, 1–21. doi: 10.1371/journal.pgen.1007378

Chan, J. J., and Tay, Y. (2018). Noncoding RNA: RNA regulatory networks in cancer. *Int. J. Mol. Sci.* 19, 1–26. doi: 10.3390/ijms19051310

Chikne, V., Rajan, K. S., Shalev-Benami, M., Decker, K., Cohen-Chalamish, S., Madmoni, H., et al. (2019). Small nucleolar RNAs controlling rRNA processing in Trypanosoma brucei. *Nucleic Acids Res.* 47, 2609–2629. doi: 10.1093/nar/gky1287

Clayton, C. E. (2014). Networks of gene expression regulation in Trypanosoma brucei. *Mol. Biochem. Parasitol.* 195, 96–106. doi: 10.1016/j.molbiopara.2014.06.005

Clayton, C. E. (2016). Gene expression in kinetoplastids. *Curr. Opin. Microbiol.* 32, 46–51. doi: 10.1016/j.mib.2016.04.018

Daigneault, M., Preston, J., Marriott, H. M., Whyte, M. K. B., and Dockrell, D. H. (2010). The identification of markers of macrophage differentiation in PMA-stimulated THP-1 cells and monocyte-derived macrophages. *PLoS One* 5, e8668. doi: 10.1371/journal.pone.0008668

De Pablos, L. M., Ferreira, T. R., Dowle, A. A., Forrester, S., Parry, E., Newling, K., et al. (2019). The mRNA-bound Proteome of Leishmania mexicana: Novel genetic insight into an ancient parasite*. *Mol. Cell. Proteomics* 18, 1271–1284. doi: 10.1074/mcp.RA118.001307

De Pablos, L. M., Ferreira, T. R., and Walrad, P. B. (2016). Developmental differentiation in Leishmania lifecycle progression: post-transcriptional control conducts the orchestra. *Curr. Opin. Microbiol.* 34, 82–89. doi: 10.1016/j.mib.2016.08.004

de Paiva, R. M. C., Grazielle-Silva, V., Cardoso, M. S., Nakagaki, B. N., Mendonça-Neto, R. P., Canavaci, A. M. C., et al. (2015). Amastin knockdown in leishmania Braziliensis affects parasite-macrophage interaction and results in impaired viability of intracellular amastigotes. *PLoS Pathog.* 11, 1–24. doi: 10.1371/journal.ppat.1005296

Dumas, C., Chow, C., Müller, M., and Papadopoulou, B. (2006). A novel class of developmentally regulated noncoding RNAs in Leishmania. *Eukaryot. Cell* 5, 2033–2046. doi: 10.1128/EC.00147-06

Engreitz, J. M., Haines, J. E., Perez, E. M., Munson, G., Chen, J., Kane, M., et al. (2016). Local regulation of gene expression by lncRNA promoters, transcription and splicing. *Nature* 539, 452–455. doi: 10.1038/nature20149

Ernst, C., and Morton, C. C. (2013). Identification and function of long non-coding RNA. *Front. Cell. Neurosci.* 7. doi: 10.3389/fncel.2013.00168

Fernandes, J. C. R., Acuña, S. M., Aoki, J. I., Floeter-Winter, L. M., and Muxel, S. M. (2019). Long non-coding RNAs in the regulation of gene expression: Physiology and disease. *Non-coding RNA* 5, 1–17. doi: 10.3390/ncrna5010017

Freitas Castro, F., Ruy, P. C., Nogueira Zeviani, K., Freitas Santos, R., Simões Toledo, J., and Kaysel Cruz, A. (2017). Evidence of putative non-coding RNAs from Leishmania untranslated regions. *Mol. Biochem. Parasitol.* 214, 69–74. doi: 10.1016/j.molbiopara.2017.04.002

Fricker, R., Brogli, R., Luidalepp, H., Wyss, L., Fasnacht, M., Joss, O., et al. (2019). A tRNA half modulates translation as stress response in Trypanosoma brucei. *Nat. Commun.* 10, 1–12. doi: 10.1038/s41467-018-07949-6

Ghildiyal, M., and Zamore, P. D. (2009). Small silencing RNAs: An expanding universe. *Nat. Rev. Genet.* 10, 94–108. doi: 10.1038/nrg2504

Gil, N., and Ulitsky, I. (2020). Regulation of gene expression by cis-acting long non-coding RNAs. *Nat. Rev. Genet.* 21, 102–117. doi: 10.1038/s41576-019-0184-5

Gilbert, W. V., Bell, T. A., and Schaening, C. (2016). Messenger RNA modifications - Form, distribution and function. *Science (80-.).* 352, 1408–1412. doi: 10.1177/0022146515594631.Marriage

Gruber, A. R., Lorenz, R., Bernhart, S. H., Neuböck, R., and Hofacker, I. L. (2008). The vienna RNA websuite. *Nucleic Acids Res.* 36, 70–74. doi: 10.1093/nar/gkn188

Guegan, F., Rajan, K. S., Bento, F., Pinto-Neves, D., Sequeira, M., Gumińska, N., et al. (2022). A long noncoding RNA promotes parasite differentiation in African trypanosomes. *Sci. Adv.* 8, 1–21. doi: 10.1126/sciadv.abn2706

Guo, H., Ingolia, N. T., Weissman, J. S., and Bartel, D. P. (2010). Mammalian microRNAs predominantly act to decrease target mRNA levels. *Nature* 466, 835–840. doi: 10.1038/nature09267

Hang, R., Deng, X., Liu, C., Mo, B., and Cao, X. (2015a). Circular RT-PCR assay using Arabidopsis samples. *Bio-Protocol* 5, 1–12. doi: 10.21769/BioProtoc.1533

Huang, H., Zhang, S., Wen, X., Sadee, W., Wang, D., Yang, S., et al. (2022). Transcription factors and ncRNAs associated with CYP3A expression in human liver and small intestine assessed with weighted gene co-expression network analysis. *Biomedicines* 10, 3061. doi: 10.3390/biomedicines10123061

Iribar, M. P., Tosi, L. R., and Cruz, A. K. (2003). A processed short transcript of Leishmania, ODD1. *Mol. Biochem. Parasitol.* 127, 205–208. doi: 10.1016/S0166-6851(03)00006-9

Junge, A., Refsgaard, J. C., Garde, C., Pan, X., Santos, A., Alkan, F., et al. (2017). RAIN: RNA-protein association and interaction networks. *Database* 2017, 1–9. doi: 10.1093/database/baw167

Kapler, G. M., Coburn, C. M., and Beverley, S. M. (1990). Stable transfection of the human parasite Leishmania major delineates a 30-kilobase region sufficient for extrachromosomal replication and expression. *Mol. Cell. Biol.* 10, 1084–1094. doi: 10.1128/mcb.10.3.1084-1094.1990

Laemmli, U. K. (1970). Cleavage of structural proteins during the assembly of the head of bacteriophage T4. *Nature* 227, 680–685. doi: 10.1038/227680a0

Lahav, T., Sivam, D., Volpin, H., Ronen, M., Tsigankov, P., Green, A., et al. (2011). Multiple levels of gene regulation mediate differentiation of the intracellular pathogen Leishmania. *FASEB J.* 25, 515–525. doi: 10.1096/fj.10-157529

Langmead, B., and Salzberg, S. L. (2012). Fast gapped-read alignment with Bowtie 2. *Nat. Methods* 9, 357–359. doi: 10.1038/nmeth.1923

Lebowitz, J. H., Smith, H. Q., Rusche, L., and Beverley, S. M. (1993). Coupling of poly (A) site selection and trans-splicing in Leishmania. *Gene Dev.* 7, 996–1007. doi: 10.1101/gad.7.6.996

Leppek, K., and Stoecklin, G. (2014). An optimized streptavidin-binding RNA aptamer for purification of ribonucleoprotein complexes identifies novel ARE-binding proteins. *Nucleic Acid Research* 42, e13. doi: 10.1093/nar/gkt956

Liang, X. H., Uliel, S., Hury, A., Barth, S., Doniger, T., Unger, R., et al. (2005). A genome-wide analysis of C/D and H/ACA-like small nucleolar RNAs in Trypanosoma brucei reveals a trypanosome-specific pattern of rRNA modification. *RNA* 11, 619–645. doi: 10.1261/rna.7174805

Liu, Z., Gutierrez-Vargas, C., Wei, J., Grassucci, R. A., Ramesh, M., Espina, N., et al. (2016). Structure and assembly model for the trypanosoma cruzi 60s ribosomal subunit. *Proc. Natl. Acad. Sci. U. S. A.* 113, 12174–12179. doi: 10.1073/pnas.1614594113

Lorenzon, L., Quilles, J. C., Campagnaro, G. D., Azevedo Orsine, L., Almeida, L., Veras, F., et al. (2022). Functional study of leishmania Braziliensis protein arginine methyltransferases (PRMTs) reveals that PRMT1 and PRMT5 are required for macrophage infection. *ACS Infect. Dis.* 8, 516–532. doi: 10.1021/acsinfecdis.1c00509

Love, M. I., Huber, W., and Anders, S. (2014). Moderated estimation of fold change and dispersion for RNA-seq data with DESeq2. *Genome Biol.* 15, 1–21. doi: 10.1186/s13059-014-0550-8

Luciano, D. J., and Belasco, J. G. (2019). Analysis of RNA 5′ ends: Phosphate enumeration and cap characterization. *Methods* 155, 3–9. doi: 10.1016/j.ymeth.2018.10.023

Malka, Y., Alkan, F., Ju, S., Körner, P. R., Pataskar, A., Shulman, E., et al. (2022). Alternative cleavage and polyadenylation generates downstream uncapped RNA isoforms with translation potential. *Mol. Cell* 82, 3840–3855.e8. doi: 10.1016/j.molcel.2022.09.036

Martínez-calvillo, S., Romero-meza, G., Vizuet-de-rueda, J. C., Floren-, L. E., Manning-cela, R., and Nepomuceno-mejía, T. (2018). Epigenetic regulation of transcription in trypanosomatid protozoa. *Current Genomics* 19, 140–149. doi: 10.2174/1389202918666170911163517

Mathews, D. H. (2014). RNA secondary structure analysis using RNAstructure. *Curr. Protoc. Bioinforma.*, 1–14. doi: 10.1002/0471250953.bi1206s46

Matthews, K. R., TsChadi, C., and Ullu, E. (1994). A common pyrimidine-rich motif governs trans-splicing and polyadenylation of tubulin polycistronic pre-mRNA in trypanosomes. *Genes Dev.* 8, 491–501. doi: 10.1101/gad.8.4.491

Mattick, J. S., Amaral, P. P., Carninci, P., Carpenter, S., Chang, H. Y., Chen, L. L., et al. (2023). Long non-coding RNAs: definitions, functions, challenges and recommendations. *Nat. Rev. Mol. Cell Biol.* 24, 430–447. doi: 10.1038/s41580-022-00566-8

Mercer, T. R., Wilhelm, D., Dinger, M. E., Soldà, G., Korbie, D. J., Glazov, E. A., et al. (2011). Expression of distinct RNAs from 3′ untranslated regions. *Nucleic Acids Res.* 39, 2393–2403. doi: 10.1093/nar/gkq1158

Meyer, K. D., Patil, D. P., Zhou, J., Zinoviev, A., Skabkin, M. A., Elemento, O., et al. (2015). 5′ UTR m6A promotes cap-independent translation. *Cell* 163, 999–1010. doi: 10.1016/j.cell.2015.10.012

Pfaffl, M. W. (2001). A new mathematical model for relative quantification in real-time RT-PCR. *Nucleic Acids Res.* 29, 2002–2007. doi: 10.1111/j.1365-2966.2012.21196.x

Putri, G. H., Anders, S., Pyl, P. T., Pimanda, J. E., and Zanini, F. (2022). Analysing high-throughput sequencing data in Python with HTSeq 2.0. *Bioinformatics* 38, 2943–2945. doi: 10.1093/bioinformatics/btac166

Queiroz, A., Sousa, R., Heine, C., Cardoso, M., Guimarães, L. H., MaChado, P. R. L., et al. (2012). Association between an emerging disseminated form of leishmaniasis and Leishmania (Viannia) Braziliensis strain polymorphisms. *J. Clin. Microbiol.* 50, 4028–4034. doi: 10.1128/JCM.02064-12

Rochette, A., McNicoll, F., Girard, J., Breton, M., Leblanc, É., Bergeron, M. G., et al. (2005). Characterization and developmental gene regulation of a large gene family encoding amastin surface proteins in Leishmania spp. *Mol. Biochem. Parasitol.* 140, 205–220. doi: 10.1016/j.molbiopara.2005.01.006

Rogers, M. B., Hilley, J. D., Dickens, N. J., Wilkes, J., Bates, P. A., Depledge, D. P., et al. (2011). Chromosome and gene copy number variation allow major structural change between species and strains of Leishmania. *Genome Res.* 21, 2129–2142. doi: 10.1101/gr.122945.111

Ruy, P. D. C., Monteiro-Teles, N. M., Miserani Magalhães, R. D., Freitas-Castro, F., Dias, L., Aquino Defina, T. P., et al. (2019). Comparative transcriptomics in Leishmania Braziliensis: disclosing differential gene expression of coding and putative noncoding RNAs across developmental stages. *RNA Biol.* 16, 639–660. doi: 10.1080/15476286.2019.1574161

Satterwhite, E. R., and Mansfield, K. D. (2022). RNA methyltransferase METTL16: Targets and function. *Wiley Interdiscip. Rev. RNA* 13, 1–21. doi: 10.1002/wrna.1681

Saxena, A., Lahav, T., Holland, N., Aggarwal, G., Anupama, A., Huang, Y., et al. (2007). Analysis of the Leishmania donovani transcriptome reveals an ordered progression of transient and permanent changes in gene expression during differentiation. *Mol. Biochem. Parasitol.* 152, 53–65. doi: 10.1016/j.molbiopara.2006.11.011

Schmidt, J. C., Manhães, L., Fragoso, S. P., Pavoni, D. P., and Krieger, M. A. (2018). Involvement of STI1 protein in the differentiation process of Trypanosoma cruzi. *Parasitol. Int.* 67, 131–139. doi: 10.1016/j.parint.2017.10.009

Shih, J. H., Chen, H. Y., Lin, S. C., Yeh, Y. C., Shen, R., Lang, Y. D., et al. (2020). Integrative analyses of noncoding RNAs reveal the potential mechanisms augmenting tumor Malignancy in lung adenocarcinoma. *Nucleic Acids Res.* 48, 1175–1191. doi: 10.1093/nar/gkz1149

Silva-Almeida, M., Pereira, B. A. S., Ribeiro-Guimarães, M. L., and Alves, C. R. (2012). Proteinases as virulence factors in Leishmania spp. infection in mammals. *Parasites Vectors* 5, 1–10. doi: 10.1186/1756-3305-5-160

Späth, G. F., and Beverley, S. M. (2001). A lipophosphoglycan-independent method for isolation of infective Leishmania metacyclic promastigotes by density gradient centrifugation. *Exp. Parasitol.* 99, 97–103. doi: 10.1006/expr.2001.4656

Tang, D., Chen, M., Huang, X., Zhang, G., Zeng, L., Zhang, G., et al. (2023). SRplot: A free online platform for data visualization and graphing. *PLoS One* 18, 1–8. doi: 10.1371/journal.pone.0294236

Ullu, E., Matthews, K. R., and Tschudi, C. (1993). Temporal order of RNA-processing reactions in trypanosomes: rapid trans splicing precedes polyadenylation of newly synthesized tubulin transcripts. *Mol. Cell. Biol.* 13, 720–725. doi: 10.1128/mcb.13.1.720

Vandesompele, J., De Preter, K., Pattyn, F., Poppe, B., Van Roy, N., De Paepe, A., et al. (2002). Accurate normalization of real-time quantitative RT-PCR data by geometric averaging of multiple internal control genes. *Genome Biol.* 3, 1–12. doi: 10.1007/s00603-018-1496-z

Walters, R. W., Matheny, T., Mizoue, L. S., Rao, B. S., Muhlrad, D., and Parker, R. (2017). Identification of NAD+ capped mRNAs in Saccharomyces cerevisiae. *Proc. Natl. Acad. Sci. U. S. A.* 114, 480–485. doi: 10.1073/pnas.1619369114

Webb, J. R., Campos-Neto, A., Skeiky, Y. A. W., and Reed, S. G. (1997). Molecular characterization of the heat-inducible LmSTI1 protein of Leishmania major. *Mol. Biochem. Parasitol.* 89, 179–193. doi: 10.1016/S0166-6851(97)00115-1

Wu, Y., El Fakhry, Y., Sereno, D., Tamar, S., and Papadopoulou, B. (2000). A new developmentally regulated gene family in Leishmania amastigotes encoding a homolog of amastin surface proteins. *Mol. Biochem. Parasitol.* 110, 345–357. doi: 10.1016/S0166-6851(00)00290-5

Wu, F., Liu, Y., Hu, S., and Lu, C. (2023). Ribosomal protein L31 (RPL31) inhibits the proliferation and migration of gastric cancer cells. *Heliyon* 9, e13076. doi: 10.1016/j.heliyon.2023.e13076

Yamashita, A., and Takeuchi, O. (2017). Translational control of mRNAs by 3'-Untranslated region binding proteins. *BMB Rep.* 50, 194–200. doi: 10.5483/BMBRep.2017.50.4.040

Zheng, L. L., Wen, Y. Z., Yang, J. H., Liao, J. Y., Shao, P., Xu, H., et al. (2013). Comparative transcriptome analysis of small noncoding RNAs in different stages of Trypanosoma brucei. *RNA* 19, 863–875. doi: 10.1261/rna.035683.112